

“© 2018 IEEE. Personal use of this material is permitted. Permission from IEEE must be obtained for all other uses, in any current or future media, including reprinting/republishing this material for advertising or promotional purposes, creating new collective works, for resale or redistribution to servers or lists, or reuse of any copyrighted component of this work in other works.”

Design Optimization of a Permanent Magnet Claw Pole Motor with Soft Magnetic Composite Cores

Bo Ma, Gang Lei, Jianguo Zhu, *Senior Member, IEEE*, Youguang Guo, *Senior Member, IEEE*

School of Electrical and Data Engineering, University of Technology, Sydney, NSW 2007, Australia

In our previous study, the claw pole motor shows promising magnetic concentrating performance for permanent magnet motors with soft magnetic composite cores. Meanwhile, its relatively complex structure also increases the core loss and cogging torque. To conduct the high dimensional optimization of the claw pole motor with comprehensive analysis models, this paper presents an improved multilevel strategy of high efficiency. Since the holistic performances, including output torque, efficiency, cogging torque and back electromotive force, are considered, an orthogonal design is utilized for the surrogate model building for increasing the optimization efficiency. A full factor sample method for the surrogate model is also conducted for comparison. The similar optimization results with the two kinds of models prove the effectiveness of the proposed method and optimal design.

Index Terms—Multilevel design optimization, orthogonal design, cogging torque, soft magnetic composite, claw pole motor.

I. INTRODUCTION

SOFT magnetic composite (SMC) material possesses many unique features compared with traditional silicon steel sheets, such as the 3D magnetic and thermal properties but low permeability and high hysteresis loss, etc. To take full advantages of the SMC material and overcome its disadvantages, lots of novel permanent magnet (PM) motor topologies of 3D magnetic field path have been investigated [1-4]. The claw pole structure (as illustrated in Fig. 1) shows promising performance on magnetic concentrating for PM motors with the material of low permeability. However, the relatively complex structure increases the partial saturation which gives rise to the core loss and cogging torque. Meanwhile, it also enhances the difficulty together with the complex performance calculation model of SMC motors.

Considering the computation burden caused by the high design dimension and comprehensive performance analysis of the PM claw pole motor (CPM), this paper proposes an improved multilevel design optimization strategy of high efficiency. In the optimization framework, the optimization is conducted in subspaces of lower design dimension. The Kriging model is also used for replacing the FEA model to increase the optimization efficiency in addition to the multilevel scheme. Compared with our research before, for the sake of reducing the computation burden further, the orthogonal design technique is utilized for sampling and building the surrogate models of the motor performances for higher efficiency. Compared with optimization with the full factor design based surrogate models, the optimal results verified the optimal design and the proposed efficient optimization approach.

II. MOTOR PERFORMANCE ANALYSIS

To conduct the optimization of the PM CPM with SMC cores, the performance analysis methods of high accuracy are introduced in this section. Due to the 3D material properties and the axial three-stack structure of the CPM, the core loss and cogging torque calculation methods are different from the traditional PM machines. Their calculation methods are introduced as below.

A. Core Loss Calculation Model

For the core loss calculation of the SMC electrical machine, the comprehensive model in the paper [2] is used here. In this model, both alternating and rotational core losses are all considered. The alternating core loss P_a is computed by

$$P_a = C_{ha} f B_p^h + C_{ea} (f B_p)^2 + C_{aa} (f B_p)^{1.5} \quad (1)$$

where f is the excitation frequency, B_p is the magnitude of the magnetic flux density, and C_{ha} , C_{ea} , C_{aa} , h are all of the alternating core loss coefficients. When the material is under two-dimensional circularly rotating flux excitation, the rotational core loss is expressed by

$$P_r = P_{hr} + C_{er} (f B_p)^2 + C_{ar} (f B_p)^{1.5} \quad (2)$$

$$\frac{P_{hr}}{f} = a_1 \left[\frac{1/s}{(a_2 + 1/s)^2 + a_3^2} - \frac{1/(2-s)}{[a_2 + 1/(2-s)]^2 + a_3^2} \right]$$

$$s = 1 - \frac{B_p}{B_s} \sqrt{1 - \frac{1}{a_2^2 + a_3^2}}$$

where P_{hr} is the hysteresis loss, B_p is the magnitude of the circular flux density; B_s is the material saturation flux density and C_{er} , C_{ar} , a_1 , a_2 , and a_3 are rotational core loss coefficients. The coefficients mentioned above can be obtained by curve fitting of the material core loss test results. With an elliptical rotating flux, the core loss can be calculated by

$$P_{er} = R_B P_r + (1 - R_B)^2 P_a \quad (3)$$

where $R_B = B_{min}/B_{maj}$, B_{min} and B_{maj} are the values of the major and minor axes of the ellipse, respectively, P_a is the alternating

Manuscript received June 27, 2017; revised September 4, 2017; accepted September 18, 2015. Corresponding author: Gang Lei (e-mail: gang.lei@uts.edu.au)

Color versions of one or more of the figures in this paper are available online at <http://ieeexplore.ieee.org>.

Digital Object Identifier (inserted by IEEE).

core loss, and P_r is the rotational core loss under two-dimensional circularly rotating flux excitation.

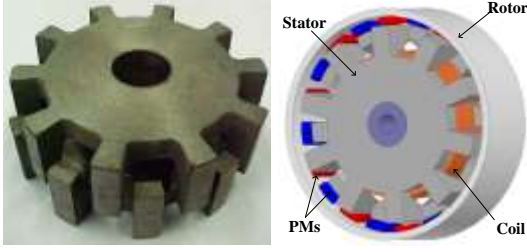


Fig. 1. Claw pole stator structure, and one phase of the PM CPM

B. Cogging Torque Calculation Model

For PM machines, cogging torque can be calculated by

$$T_c = \frac{\partial W}{\partial \theta} \quad (4)$$

where W means the co-energy, and θ is the rotor angular displacement. To analyze the cogging torque of the whole machine with three stacks, discrete Fourier transformation (DFT) is used for decomposing the cogging torque of each stack. As presented in Fig. 2(a) the cogging torque of one phase has a period of 18° mechanical and anti-symmetry about zero. Therefore, only even sine harmonics exist after the DFT

$$T_{Ac} \approx 0.615 \sin 2\theta + 0.0629 \sin 4\theta - 0.127 \sin 6\theta + \dots \quad (5)$$

where T_{Ac} means the cogging torque of stack A as shown in Fig. 2(b). Because of 120 electrical-degree displacements of each stack only 6^{th} and its multiple harmonics left in the whole machine, which can be expressed as

$$T_{cog} = T_{Ac} + T_{Bc} + T_{Cc} = c_{k1} \sin 6\theta + c_{k2} \sin 12\theta + \dots \quad (6)$$

where c_{k1} and c_{k2} are the coefficients obtained from DFT, T_{Bc} and T_{Cc} are the cogging torque of stack B and C, respectively.

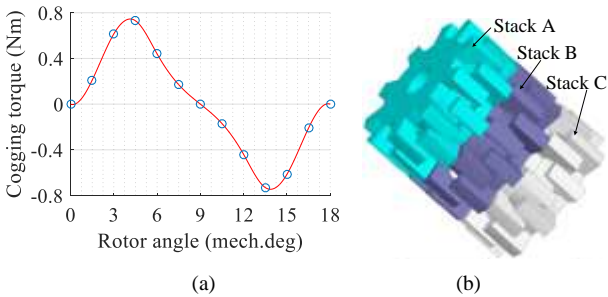


Fig. 2. (a) Cogging torque of one phase, (b) three stator stack with 120 electrical-degree displacements. (mech.deg stands for mechanical degree)

Fig. 3 illustrates the waveform of the back electromotive force (EMF) and the cogging torque calculated by the proposed method, which are verified by the experiment. The calculated and measured values are listed in Table I, which verify the accuracy of the performance analysis models. Specially, the back EMF constant means the value of back electromotive force divided by the speed.

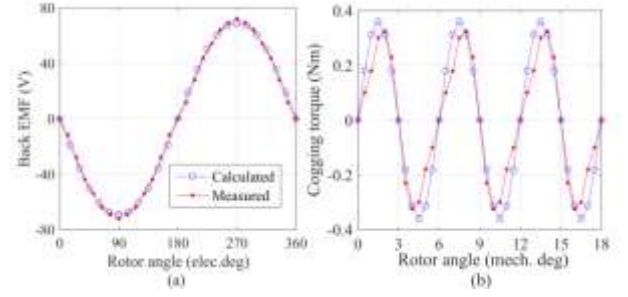


Fig. 3. Calculated and measured performances for the CPM, (a) back EMF, (b) cogging torque. (elec.deg stands for electrical degree)

TABLE I
KEY PERFORMANCE VALIDATION OF THE INITIAL DESIGN

Par.	Unit	Calculated	Measured
Back EMF constant	V/rpm	0.0272	0.0271
No load core loss	W	58	60
Cogging torque	Nm	0.35	0.33

III. MULTILEVEL DESIGN OPTIMIZATION

Fig. 4 illustrates the structure design parameters, and the whole optimization dimension is more than ten. If taking all the parameters into consideration at the same time, the computation burden can be very huge. Moreover, for each design usually half or whole periodic points need to be calculated. Take the cogging torque calculation as an example. Usually 12 points are computed by FEA for the DFT analysis. The similar computation with periodic points should also be conducted for the back EMF. For decreasing the computation burden, a multilevel optimization scheme combined with orthogonal design method is presented in this section.

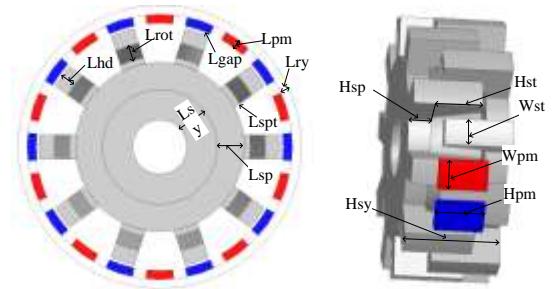


Fig. 4. Main structure design parameters in three dimensions

A. Multilevel Optimization Scheme

The multilevel optimization method has two main implementation steps [5]. Firstly, divide the initial high dimensional design space into three low dimensional subspaces regarding the significance order of all parameters. Secondly, optimize these subspaces sequentially till convergence criterion is met.

The division of the optimization levels is according to the sensitivity of each parameter. In this work, the local sensitivity analysis method is used and the sensitivity is calculated as

$$S_i = \frac{F(\mathbf{x}_0 \pm \Delta \mathbf{x}_i) - F(\mathbf{x}_0)}{\pm \Delta \mathbf{x}_i} \quad (7)$$

where $F(\mathbf{x})$ is the objective function, and \mathbf{x} is the design parameter vector. Δx_i is the increment of parameter x_i .

Since the cogging torque reduction is also considered, the sensitivity is calculated according to the function

$$F(\mathbf{x}) = \eta_{initial} / \eta + T_{ave_initial} / T_{ave} + T_{cog} / T_{cog_initial} \quad (8)$$

where T_{cog} and T_{ave} are the cogging torque and output torque respectively, η is the motor efficiency at rate point. The subscript *initial* means the initial value of the prototype performance. Table II lists the selected design parameters and their sensitivities after the local sensitivity analysis. Table III lists the design parameters in each level.

TABLE II
INITIAL DESIGN OF THE CPM

Par.	Description	Unit	Initial	Sen.
L_{sy}	Length of stator yoke	mm	10	0.013
L_{sp}	Length of stator plate	mm	10	0.034
L_{spt}	Length between plate and teeth	mm	1	0.013
L_{rot}	Length of tooth root	mm	5	0.016
L_{hd}	Length of tooth head	mm	5	0.026
L_{gap}	Length of air gap	mm	1	0.079
W_{st}	tooth circumferential width	mm	8	0.206
W_{pm}	PM circumferential width	deg	12	0.198
H_{sy}	Height of stator yoke	mm	31	0.012
H_{sp}	Height of stator plate	mm	7	0.028
H_{st}	Height of tooth	mm	14.35	0.067
H_{pm}	Height of PM	mm	15	0.031
Br	Remanence of PM	T	1.15	0.073
D	Diameter of copper wire	mm	1	0.005
N	Turns of coil	-	75	0.084

Sen. stands for sensitivity

TABLE III
DESIGN PARAMETERS IN EACH LEVEL

Level Num.	Design parameters
Level 1	$W_{st}, W_{pm}, N, L_{gap}$
Level 2	$Br, H_{st}, L_{sp}, H_{pm}, H_{sp}$
Level 3	$L_{sy}, L_{spt}, L_{rot}, L_{hd}, H_{sy}, D$

B. Approximation Model Building with Orthogonal Design

Kriging model is used as the surrogate model of FEM to reduce the computation cost [5, 6]. For the sake of calculating the cogging torque and back EMF, two separately computation processes with FEM are needed. Both of them contain the FEA points of half or whole period, respectively. For example, for a 4-factor-5-level experiment, 625 samples are needed according to the full factor experiment. If each of the cogging torque calculation contains 6 FEA points, the whole FEA points will be $2 \times 6 \times 625$, i.e., 7500. Thus, the orthogonal experiment design technique is taken here for reducing the design space [7, 8]. For example, for a 4-factor-9-level experiment, only 81 samples are needed by orthogonal design technique, which offers an effective way for reducing the sample dimension along with the multilevel method.

To be more specific, for the motor design problem, the orthogonal design with high level (more than 9) is suggested to compensate the lacking of sample points. For CPM optimization problem, there are 15 parameters and three subspaces in total. Since the diameter of copper wire (D) does not need to be sampled by FEA, the 4 factor 13 level orthogonal array and 5 factor 17 level orthogonal array are used, and the sample numbers are 169 and 289, respectively.

C. Optimization Model

Based on the above analysis methods, the optimization model can be developed for this CPM. The optimization purpose is defined as increasing the output torque and efficiency. Meanwhile, the cogging torque and total harmonic distortion (THD) of back EMF are controlled lower than the setting values. Therefore, the optimization model can be expressed as

$$\begin{aligned} \min : f(\mathbf{x}) &= \frac{\eta_{initial}}{\eta} + \frac{T_{ave_initial}}{T_{ave}} \\ \text{s.t.} \quad &\begin{cases} g_1(\mathbf{x}) = T_{ave_initial} - T_{ave} \leq 0, g_2(\mathbf{x}) = 0.815 - \eta \leq 0, \\ g_3(\mathbf{x}) = Cost - Cost_{initial} \leq 0, g_4(\mathbf{x}) = sf - 0.7 \leq 0, \\ g_5(\mathbf{x}) = T_{cog} - 0.05T_{ave} \leq 0, \\ g_6(\mathbf{x}) = THD(E) - 0.03 \leq 0 \end{cases} \end{aligned} \quad (9)$$

where $Cost$ is the material and stator core manufacturing price, and $THD(E)$ is the THD of the back EMF curve. In addition to the objectives and constraints mentioned above, the output torque, efficiency and cost are required to be better than the initial values. Meanwhile, the slot fill (sf) factor should be less than 0.7 for manufacturing requirement.

IV. RESULTS AND DISCUSSION

For proving the effectiveness of the improved method, this paper conducted the multilevel optimization based on two Kriging models sampled according to the full factor and orthogonal designs, respectively. The optimization based on both models was conducted with the same differential evolution algorithm. Please note the results below with title or legend of full factor or orthogonal mean the optimization results obtained with Kriging models built by the two designs respectively.

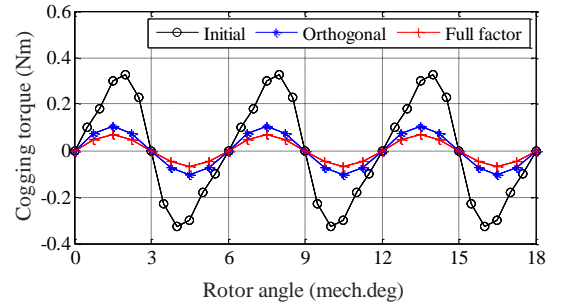


Fig. 5. Cogging torque comparison among different designs

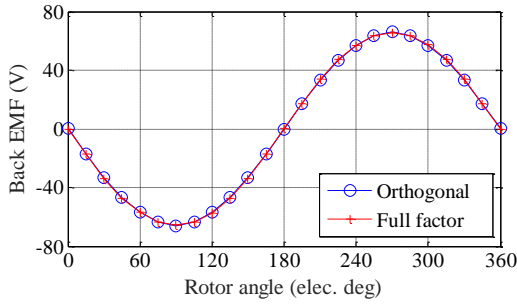


Fig. 6. Back EMF comparison between two designs

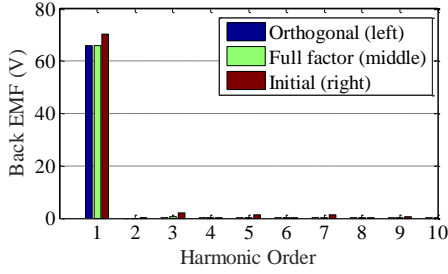


Fig. 7. Comparison of the harmonic order of the back EMF

TABLE IV
OPTIMAL PERFORMANCES COMPARISON

Performance	Initial	Full factor	Orthogonal
Torque (Nm)	2.65	3.09	3.06
efficiency	0.815	0.839	0.841
Cogging torque (Nm)	0.33	0.068	0.103

TABLE V
SAMPLING NUMBER COMPARISON

Level Num.	Full factor	Orthogonal
Level 1	625	169
Level 2	1024	289
Level 3	1024	289
Sum	2673	747

According to the optimization results, we can draw the following conclusions.

1. The final optimal solution $\mathbf{x} = [10.88, 10.97, 0.85, 5.75, 3, 1.16, 6.35, 11.45, 31.15, 10.95, 7.65, 12.75, 1.39, 1.25, 74]$, based on the Kriging model with orthogonal design, is of the small difference with the solution from full factor design, $\mathbf{x} = [10.88, 11.81, 0.9, 5.7, 3, 1.16, 6.4, 11.4, 31.12, 10.25, 8.2, 12.3, 1.39, 1.25, 74]$, according to the order $\mathbf{x} = [L_{sy}, L_{sp}, L_{spt}, L_{rot}, L_{hd}, L_{gap}, W_{st}, W_{pm}, H_{sy}, H_{st}, H_{sp}, H_{pm}, Br, D, N]$. As listed in Table IV, the optimal objective performances of output torque and efficiency are similar with maximal errors. As illustrated in Fig. 5, the waveforms of the cogging torque of the optimal solutions are verified by FEA. Even though the cogging torque optimization results show difference, both of them are under the constraints defined in the optimization model.
2. Fig. 6 illustrates the verification results back EMF waveform by the FEA. The waveforms of the two

optimization results are almost aligned. The harmonic analysis result shown in Fig. 7 proves the very low harmonic content and the THD analysis result is much lower than the set value 3%.

3. Table V lists the comparison of the sample numbers of the full factor and orthogonal design methods for the modeling of Kriging. The total FEM sample number required by improved multilevel optimization strategy with orthogonal design is 747, which is only 27.95% (747/2673) of the full factor sampling method.

As the result listed above, the proposed method shows high effectiveness in both reducing the computational burden while keeping the accuracy of the performance calculation.

V. CONCLUSION

The high design dimension and complete performance analysis cause the heavy computation burden when conducting optimization of the PM CPM. To solve this problem effectively, the improved multilevel design optimization method with orthogonal sampling proposed shows high potential. The computation burden of the optimization is decreased further by the efficient sampled surrogate modeling, with the dimension reduced multilevel optimization framework. Therefore, the design optimization cycle can be shortened effectively by using the proposed approach.

ACKNOWLEDGMENT

This work was supported in part by the China Scholarship Council under Grant 201506690023 and Postdoctoral Science Foundation projects 2013M540578 and 2014T70699.

REFERENCES

- [1] Y. S. Kwon and W. J. Kim, "Electromagnetic analysis and steady-state performance of double-sided flat linear motor using soft magnetic composite," *IEEE Trans. Ind. Electron.*, vol. 64, no. 3, pp. 2178-87, 2017.
- [2] Y. G. Guo, J. G. Zhu, and H. Y. Lu, "Accurate determination of parameters of a claw-pole motor with SMC stator core by finite-element magnetic-field analysis," *IEE Proceedings - Electric Power Applications*, vol. 153, pp. 568-574, 2006.
- [3] Y. G. Guo, J. G. Zhu, Z. W. Lin and J. J. Zhong, "Measurement and modeling of core losses of soft magnetic composites under 3-D magnetic excitations in rotating motors," in *IEEE Trans. Magn.*, vol. 41, no. 10, pp. 3925-3927, Oct. 2005.
- [4] B. Zhang, T. Seidler, R. Dierken, and M. Doppelbauer, "Development of a yokeless and segmented armature axial flux machine," *IEEE Trans. Ind. Electron.*, vol. 63, no. 4, pp. 2062-2071, 2016.
- [5] G. Lei, C. Liu, J. Zhu and Y. Guo, "Techniques for multilevel design optimization of permanent magnet motors," *IEEE Trans. Energy Convers.*, vol. 30, no. 4, pp. 1574-1584, Dec. 2015.
- [6] L. Lebensztajn, C.A.R. Marretto, M. C. Costa, and J. L. Coulomb, "Kriging: a useful tool for electromagnetic device optimization," *IEEE Trans. Magn.*, vol. 40, no. 2, pp. 1196-1199, 2004.
- [7] G. Lei, Y. G. Guo, J. G. Zhu, X. M. Chen, W. Xu, and K. R. Shao, "Sequential subspace optimization method for electromagnetic devices design with orthogonal design technique," *IEEE Trans. Magn.*, vol. 48, pp. 479-482, 2012.
- [8] [Online]. Available: <http://neilsloane.com/oadir/>